tion in order to obtain accurate numerical results. We can also obtain, by means of (36), the higher order modes. In this case the integrals which express the equation coefficients must be regarded as principal values since function $\Delta(k)$ vanishes inside the integration domain.

V. Conclusions

A new method is given for calculating the dispersion characteristics of microstrip lines. The analysis is rigorous and it expresses the solution of the dispersion equation in terms of the solution of a double infinite system of linear equations. The system coefficients are given by certain quadratures. The numerical examples reveal the high convergence order of the method.

References

[1] H. A. Wheeler, "Transmission-line properties of parallel strips separated by dielectric sheet," *IEEE Trans. Microwave Theory Tech.*, vol. MTT-13, pp. 172–185, Mar 1965.

[2] E. Yamashita and R. Mittra, "Variational method for the analysis of microstrip lines," *IEEE Trans. Microwave Theory Tech.*, vol. MTT-16, pp. 251–256, Apr. 1968.

[3] P. Silvester, "TEM wave properties of microstrip transmission lines," *Proc. Inst. Elec. Eng.*, vol. 115, pp. 43–48, Jan. 1968.

[4] D. Homentcovschi, A. Manolescu, A. M. Manolescu, and L. Kreindler, "An analytical solution for the coupled stripline-like microstrip line problem," *IEEE Trans. Microwave Theory Tech.*, vol. 36, pp. 1002–1007, June 1988.

[5] E. J. Denlinger, "A frequency dependent solution for microstrip transmission lines," *IEEE Trans. Microwave Theory Tech.*, vol. MTT-19, pp. 30–39, Jan. 1971.

[6] J. S. Hornsby and A. Gopinath, "Numerical analysis of a dielectric-loaded waveguide with a microstrip line—Finite difference method," *IEEE Trans. Microwave Theory Tech.*, vol. MTT-17, pp. 684–690, Sept. 1969.

[7] P. Daly, "Hybrid-mode analysis of microstrip by finite element methods," *IEEE Trans. Microwave Theory Tech.*, vol. MTT-19, pp. 19–25, Jan. 1971.

[8] G. I. Zysman and D. Varon, "Wave propagation in microstrip transmission lines," in *1969 IEEE MTT-S Int. Microwave Symp. Dig.* (Dallas, TX), pp. 3–9.

[9] E. Yamashita and K. Atuski, "Analysis of microstrip-like transmission lines by nonuniform discretization of integral equations," *IEEE Trans. Microwave Theory Tech.*, vol. MTT-24, pp. 195–200, Apr. 1976.

[10] R. Mittra and T. Itoh, "A new technique for the analysis of the dispersion characteristics of microstrip lines," *IEEE Trans. Microwave Theory Tech.*, vol. MTT-19, pp. 47–56, Jan. 1971.

[11] T. Itoh and R. Mittra, "Spectral domain approach for calculating the dispersion characteristics of microstrip-lines," *IEEE Trans. Microwave Theory Tech.*, vol. MTT-21, pp. 496–499, July 1973.

[12] M. Kobayashi and F. Ando, "Dispersion characteristics of open microstrip lines," *IEEE Trans. Microwave Theory Tech.*, vol. MTT-35, p. 105, Feb. 1987.

[13] N. Fache and D. De Zutter, "Rigorous full-wave space domain solution for dispersive microstrip lines," *IEEE Trans. Microwave Theory Tech.*, vol. 36, pp. 731–737, Apr. 1988.

[14] K. Uchida, T. Noda, and T. Tatsunga, "New type of spectral-domain analysis of a microstrip line," *IEEE Trans. Microwave Theory Tech.*, vol. 37, pp. 947–952, June 1989.

[15] C. Shin, R. B. Wu, S. K. Jeng, and C. H. Chen, "A full wave analysis of microstrip lines by variational conformal mapping technique," *IEEE Trans. Microwave Theory Tech.*, vol. 36, pp. 576–581, Mar. 1988.

[16] E. F. Kuester and D. C. Chang, "An appraisal of methods for computation of the dispersion characteristics of open microstrip," *IEEE Trans. Microwave Theory Tech.*, vol. MTT-27, pp. 691–694, 1979.

[17] R. F. Harrington, *Time-Harmonic Electromagnetic Fields*. New York: McGraw-Hill, 1961.

[18] D. Homentcovschi, "An analytical solution for the microstrip line problem," *IEEE Trans. Microwave Theory Tech.*, vol. 38, pp. 766–769, June 1990.

Admittance Calculation of a Slot in the Shield of a Multiconductor Transmission Line

Richard G. Plumb

Abstract—**The admittance calculation for a narrow slot in the conducting shield of a multiconductor transmission line is presented. The admittance represents a generalized admittance resulting from an asymptotic, one-term moment method solution and is approximated using transmission line theory. The calculated admittance is useful in modeling connectors for multiconductor transmission lines. Some useful impedance calculations for multiconductor transmission lines are developed.**

I. Introduction

In a recent paper [1], we presented a method of modeling connectors for multiconductor transmission lines (MTL's). In that investigation the connector was modeled as a narrow circumferential slot, of width d, in the shield of an MTL. The MTL, uniform in the axial direction and having an arbitrary cross section, contained N lines and a conducting shield of finite width t. The interior medium of the MTL was assumed lossless and homogeneous. The problem was solved by treating the slot as a thick aperture in the shield. The equivalence principle was invoked to obtain two coupled integral equations in the equivalent surface magnetic currents. A one-term moment method solution was then obtained for an electrically narrow slot and a small shield radius. The moment method solution led to an equivalent circuit representation. Power calculations were derived from the equivalent circuit for the power radiated through the slot and the power transmitted down the line. When the slot admittance is replaced by the transfer admittance of a connector, the power radiated through the slot becomes the power radiated through the connector.

The original MTL network and an equivalent circuit are shown in Fig. 1. The equivalent circuit consists of the admittances Y^a, Y^b, and Y^c, corresponding to the generalized admittance of the internal region of the MTL, the slot region, and the region external to the MTL respectively. For a one-term moment method solution, Y^c is the radiation admittance or the external input admittance of the antenna formed by the outer shield surface, having a finite feed width of length d, when a uniform electric field excites the antenna. The admittance Y^b corresponds to the transfer admittance of the slot, which can be interpreted as the transfer admittance of a connector. The current source I^i is a generalized current source and is obtained by calculating the net short circuit shield current on the inner shield surface. The current I^i is the current on the inner shield surface when the slot is covered with a perfect conductor.

In this paper we detail the calculations for the admittance Y^a. An approximate expression for the admittance is obtained using transmission line theory. In doing so, some useful impedance calculations for multiconductor transmission lines are presented.

II. Statement of the Problem

The admittance Y^a is the admittance at the inner slot surface looking into the MTL when a uniform magnetic current is placed over the shorted surface [2]. The magnitude of the

Manuscript received May 17, 1990; revised November 19, 1990.

The author is with the Department of Electrical and Computer Engineering, University of Kansas, Lawrence, KS 66045-2969.

IEEE Log Number 9042497.

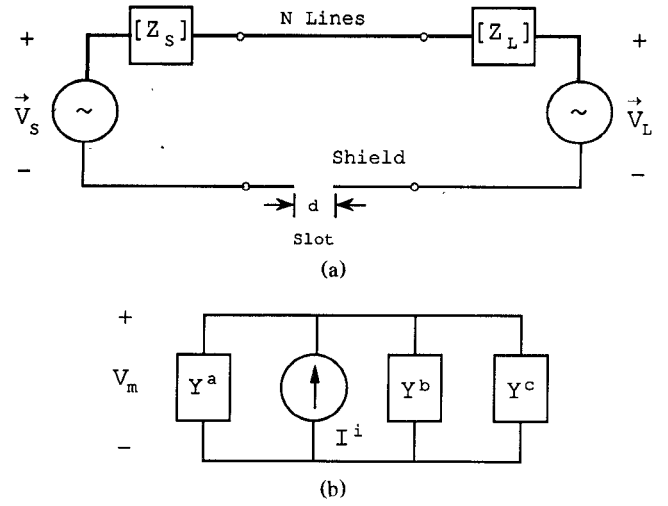

Fig. 1. (a) Original MTL network including terminations and (b) an equivalent circuit for the slot region.

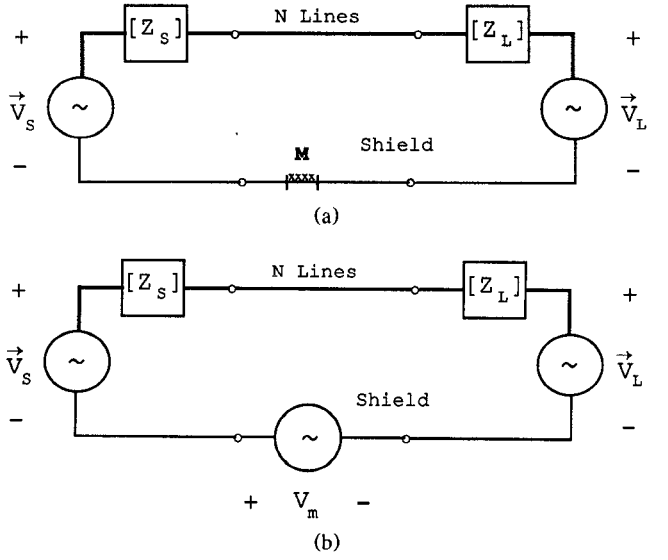

Fig. 2. An equivalent network for the interior of the MTL network of Fig. 1(a) with (a) a magnetic current over the slot and (b) a point voltage source.

magnetic current M, shown in Fig. 2(a), is equal to the magnitude of the original electric field at the inner slot surface when the slot is present. The effect of the magnetic current is to produce the same field distribution inside the MTL as in the original problem. The field distributions inside the MTL of Figs. 1(a) and 2(a) are, therefore, identical. When βd is small, where β is the wavenumber inside the MTL, the effect of this magnetic current is essentially that of a point voltage source V_m driving the shield as seen in Fig. 2(b). By neglecting all higher order modes, Y^a is approximately given by the driving point admittance of the voltage source and can be calculated from transmission line theory.

The problem we consider here then is the calculation of the driving point admittance of a voltage source located in the shield of an MTL as shown in Fig. 2(b). The terminating networks in Fig. 2 are represented by equivalent Thevenin

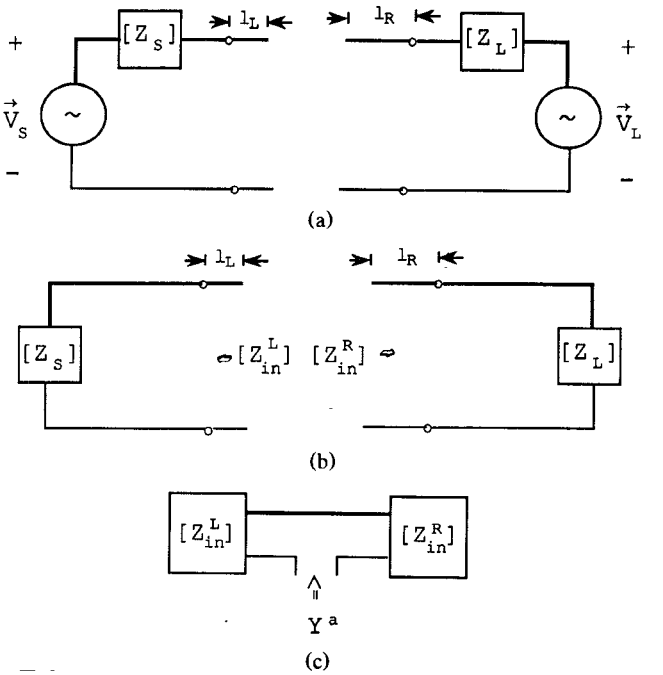

Fig. 3. Steps required in calculating Y^a. (a) Divide the MTL network in two, (b) compute the input impedance matrices of the N-ports, and (c) create a 1-port from the two N-ports.

networks and are assumed known. The voltage sources in the Thevenin networks represented the impressed sources, which are independent sources, while the voltage source in the shield is a dependent source. The driving point admittance, which is given by the ratio of the net shield current to the voltage V_m, is calculated as follows. Divide the MTL network of Fig. 2 in two at the location of the source V_m as shown in Fig. 3(a). By using the matrix chain parameters, compute the impedance looking into the two newly created N-ports with all sources deactivated, as shown in Fig. 3(b). Then, using standard network theory, compute the driving point admittance of the 1-port formed by the connection of the two N-ports as depicted in Fig. 3(c).

III. Analysis

The input impedance of the two N-ports of Fig. 3(a) can easily be obtained by using the matrix chain parameters for MTL's. A brief review of the matrix chain parameters (or *ABCD* parameters) will be given here [3].

Consider the uniform, homogeneous MTL network containing $N+1$ lines as shown in Fig. 4. The line voltages and currents are represented by the vectors $\vec{V}(x)$ and $\vec{I}(x)$. Under time-harmonic conditions, the line voltage and current vectors satisfy the state variable equation

$$\begin{bmatrix} \dfrac{d\vec{V}(x)}{dx} \\ \dfrac{d\vec{I}(x)}{dx} \end{bmatrix} = \begin{bmatrix} [0] & -[Z] \\ -[Y] & [0] \end{bmatrix} \begin{bmatrix} \vec{V}(x) \\ \vec{I}(x) \end{bmatrix} \tag{1}$$

where $[Z]$ and $[Y]$ are the $N \times N$ per-unit-length impedance and admittance matrices of the MTL and $[0]$ is an $N \times N$ matrix with all elements equal to zero. The solution to (1) is

$$\begin{bmatrix} \vec{V}(x) \\ \vec{I}(x) \end{bmatrix} = [\phi(x - x_0)] \begin{bmatrix} \vec{V}(x_0) \\ \vec{I}(x_0) \end{bmatrix}, \qquad x \geq x_0 \tag{2}$$

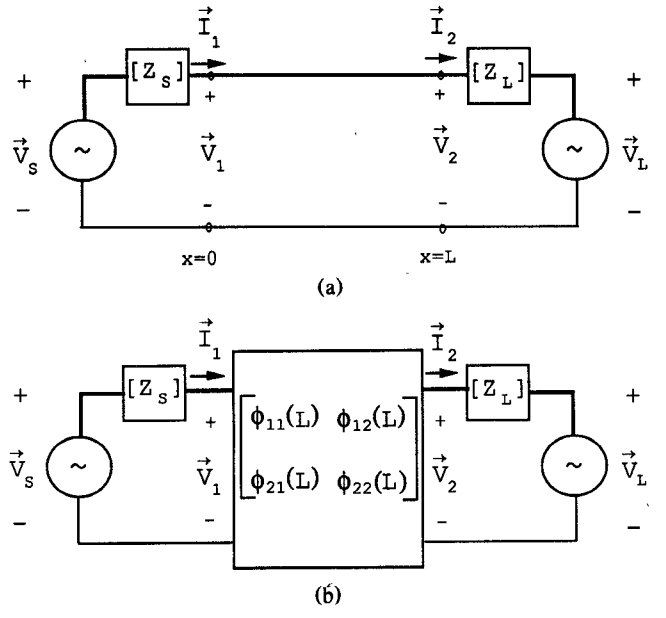

Fig. 4. (a)A uniform MTL of length L with Thevenin equivalent networks for terminations and (b) a $2N$-port representation of the section of MTL.

where x_0 is a reference point and $[\phi(x-x_0)]$ is the $2N\times 2N$ state transition matrix, or the chain parameter matrix, given by

$$[\phi(x-x_0)]=\begin{bmatrix}[\phi_{11}(x-x_0)] & [\phi_{12}(x-x_0)]\\ [\phi_{21}(x-x_0)] & [\phi_{22}(x-x_0)]\end{bmatrix}. \quad (3)$$

The $[\phi_{ij}]$ in (3) are $N\times N$ submatrices and are [3]

$$[\phi_{11}(x-x_0)]=\cosh\left\{\sqrt{[Z][Y]}\,(x-x_0)\right\} \quad (4)$$

$$[\phi_{12}(x-x_0)]=-\sinh\left\{\sqrt{[Z][Y]}\,(x-x_0)\right\}[Z_c] \quad (5)$$

$$[\phi_{21}(x-x_0)]=-[Z_c]^{-1}\sinh\left\{\sqrt{[Z][Y]}\,(x-x_0)\right\} \quad (6)$$

$$[\phi_{22}(x-x_0)]=[Y]\cosh\left\{\sqrt{[Z][Y]}\,(x-x_0)[Y]^{-1}\right. \quad (7)$$

where $[Z_c]$ is the characteristic impedance of the MTL, defined as

$$[Z_c]=\sqrt{[Z][Y]}\,[Y]^{-1} \quad (8a)$$

or, equivalently,

$$[Z_c]=\left(\sqrt{[Z][Y]}\right)^{-1}[Z]. \quad (8b)$$

For lossless lines, $[Z]$ and $[Y]$ are

$$[Z]=j\omega[L] \quad (9)$$

$$[Y]=j\omega[C] \quad (10)$$

where $[L]$ and $[C]$ are the per-unit-length external inductance and capacitance matrices. For lossless, homogeneous lines, (4)–(8) reduce to

$$[\phi_{11}(x-x_0)]=\cos\{\beta(x-x_0)\}[I] \quad (11)$$

$$[\phi_{12}(x-x_0)]=\frac{-j\omega}{\beta}\sin\{\beta(x-x_0)\}[L] \quad (12)$$

$$[\phi_{21}(x-x_0)]=\frac{-j\beta}{\omega}\sin\{\beta(x-x_0)\}[L]^{-1} \quad (13)$$

$$[\phi_{22}(x-x_0)]=\cos\{\beta(x-x_0)[I] \quad (14)$$

$$[Z_c]=\frac{\omega}{\beta}[L] \quad (15)$$

where $[I]$ is the $N\times N$ identity matrix and β is the wavenumber.

From (2) the voltages and currents at any point along the MTL are known in terms of the chain matrix parameters and the voltages and currents at the reference point x_0. By taking the reference point x_0 equal to zero and x equal to the line length, the MTL network of Fig. 4(a) can be represented by the $2N$-port of Fig. 4(b). The chain matrix parameters relate the output voltage and current vectors to the input vectors as

$$\begin{bmatrix}\vec{V}_2\\ \vec{I}_2\end{bmatrix}=\begin{bmatrix}[\phi_{11}(L)] & [\phi_{12}(L)]\\ [\phi_{21}(L)] & [\phi_{22}(L)]\end{bmatrix}\begin{bmatrix}\vec{V}_1\\ \vec{I}_1\end{bmatrix}. \quad (16)$$

The termination conditions are given by Kirchhoff's law as

$$-\vec{V}_s+[Z_s]\vec{I}_1+\vec{V}_1=\vec{0}_N \quad (17)$$

$$-\vec{V}_2+[Z_L]\vec{I}_2+\vec{V}_L=\vec{0}_N \quad (18)$$

where $\vec{0}_N$ is a vector containing N zeros. Solving (17) and (18) for $\vec{V}_1$ and $\vec{V}_2$ yields

$$\vec{V}_1=\vec{V}_s-[Z_s]\vec{I}_1 \quad (19)$$

$$\vec{V}_2=\vec{V}_L+[Z_L]\vec{I}_2. \quad (20)$$

Equation (16) can now be solved for the input voltage and current vectors subject to (19) and (20). With the input vectors known, the voltages and currents along the line are simply given by (2).

The input impedance of the two N-ports of Fig. 3(c) can be computed using the chain matrix parameters. First consider the section of MTL of length l_L terminated in an impedance network $[Z_s]$ as shown in Fig. 5. From (2), the voltages and currents are related as

$$\begin{bmatrix}\vec{V}_2\\ \vec{I}_2\end{bmatrix}=\begin{bmatrix}[\phi_{11}(l_L)] & [\phi_{12}(l_L)]\\ [\phi_{21}(l_L)] & [\phi_{22}(l_L)]\end{bmatrix}\begin{bmatrix}\vec{V}_1\\ \vec{I}_1\end{bmatrix}. \quad (21)$$

The output termination condition is

$$\vec{V}_1=-[Z_s]\vec{I}_1. \quad (22)$$

An expression relating the input voltage $\vec{V}_2$ to the input current $\vec{I}_2$ is desired.

Substituting (22) into the second equation of (21) and solving for $\vec{I}_1$ gives

$$\vec{I}_1=([\phi_{22}(l_L)]-[\phi_{21}(l_L)][Z_s])^{-1}\vec{I}_2. \quad (23)$$

Combining (22) and (23) with the first equation of (21) and solving for $\vec{V}_2$ shows

$$\vec{V}_2=([\phi_{12}(l_L)]-[\phi_{11}(l_L)][Z_s])\cdot([\phi_{22}(l_L)]-[\phi_{21}(l_L)][Z_s])^{-1}\vec{I}_2. \quad (24)$$

The desired input impedance is then seen as

$$[Z_{\text{in}}^{l_L}]=-([\phi_{12}(l_L)]-[\phi_{11}(l_L)][Z_s])\cdot([\phi_{22}(l_L)]-[\phi_{21}(l_L)][Z_s])^{-1}. \quad (25)$$

Now consider another section of MTL of length l_R. Let the opposite end be terminated in the load $[Z_L]$. The output termination condition is

$$\vec{V}_2=[Z_L]\vec{I}_2. \quad (26)$$

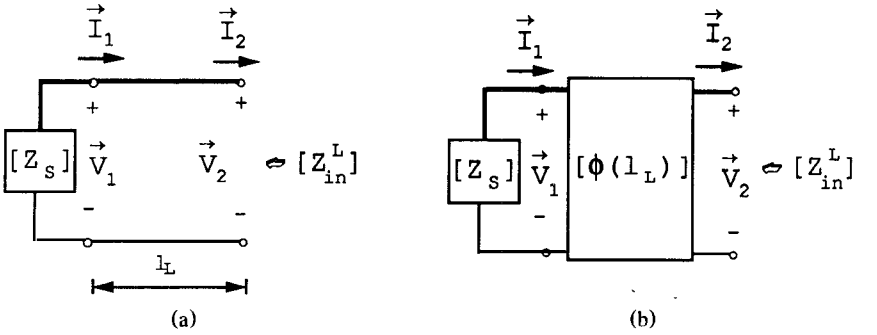

Fig. 5. Input impedance of an MTL with its input terminated in an impedance matrix $[Z_s]$. (a) Transmission line representation and (b) chain matrix representation.

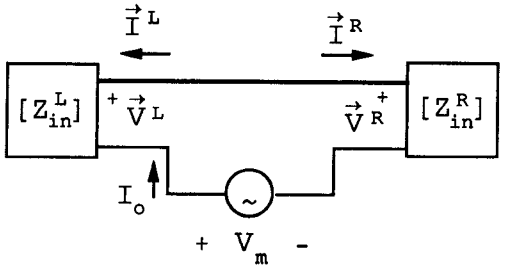

Fig. 6. Circuit used to compute the driving point admittance.

A similar analysis shows that the desired input impedance is

$$[Z_{in}^R] = -([\phi_{11}(l_R)] - [Z_L][\phi_{21}(l_R)])^{-1} \cdot ([\phi_{12}(l_R)] - [Z_L][\phi_{22}(l_R)]). \quad (27)$$

For lossless lines it is easy to show, with the aid of (11)–(14), that the above equations reduce to

$$[Z_{in}^L] = ([Z_s] + j\tan(\beta l_L)[Z_c]) \cdot ([Z_c] + j\tan(\beta l_L)[Z_s])^{-1}[Z_c] \quad (28)$$

$$[Z_{in}^R] = [Z_c]([Z_c] + j\tan(\beta l_R)[Z_L])^{-1} \cdot ([Z_L] + j\tan(\beta l_R)[Z_c]). \quad (29)$$

Equations (28) and (29) are the extension of the familiar input impedance of a two-conductor line.

The admittance Y^a is approximated by the driving point admittance of the 1-port formed by the connection of the two N-ports as shown in Fig. 3. To determine Y^a, place a voltage source V_m across the terminals of the 1-port of Fig. 3(c) as shown in Fig. 6. The driving point admittance of the voltage source is the ratio of the current I_0 to the voltage V_m [4]:

$$Y^a = I_0 / V_m. \quad (30)$$

Define an N-element voltage vector $\vec{V}_m$ as

$$\vec{V}_m = V_m(1\ 1 \cdots 1). \quad (31)$$

Kirchhoff's voltage and current laws for the 1-port may be expressed as

$$-\vec{V}^R + \vec{V}^L + \vec{V}_m = \vec{0}_N \quad (32)$$

$$\vec{I}^R + \vec{I}^L = \vec{0}_N \quad (33)$$

where $\vec{V}^R$ and $\vec{I}^R$, and $\vec{V}^L$ and $\vec{I}^L$ are the N-element terminal voltage and current vectors of the two N-ports. Assuming the two N-ports to be linear and passive, the sum of the currents entering them is zero, or

$$\sum_{n=1}^{N} I_n^L + I_0 = 0 \quad (34)$$

$$\sum_{n=1}^{N} I_n^R - I_0 = 0. \quad (35)$$

The terminal relations for the two N-ports are

$$\vec{V}^R = [Z_{in}^R]\vec{I}^R \quad (36)$$

$$\vec{V}^L = [Z_{in}^L]\vec{I}^L. \quad (37)$$

Combining (32), (33), (36), and (37) and solving for $\vec{I}^L$ shows

$$\vec{I}^L = -([Z_{in}^R] + [Z_{in}^L])^{-1}\vec{V}_m. \quad (38)$$

Let $([Z_{in}^R]+[Z_{in}^L])_{ij}^{-1}$ denote the ijth element of the inverse of the matrix $([Z_{in}^R]+[Z_{in}^L])$. Then the N equations of (38) may be rewritten as

$$I_1^L = -\sum_{n=1}^{N} ([Z_{in}^R] + [Z_{in}^L])_{1n}^{-1} V_m$$

$$I_2^L = -\sum_{n=1}^{N} ([Z_{in}^R] + [Z_{in}^L])_{2n}^{-1} V_m$$

$$\vdots$$

$$I_N^L = -\sum_{n=1}^{N} ([Z_{in}^R] + [Z_{in}^L])_{Nn}^{-1} V_m. \quad (39)$$

Summing the N equations of (39) and using (34) gives

$$I_0 = \sum_{i=1}^{N}\sum_{j=1}^{N} ([Z_{in}^R] + [Z_{in}^L])_{ij}^{-1} V_m. \quad (40)$$

Therefore the desired driving point admittance is given by

$$Y^a = \sum_{i=1}^{N}\sum_{j=1}^{N} ([Z_{in}^R] + [Z_{in}^L])_{ij}^{-1}. \quad (41)$$

IV. Summary

In this paper we presented an approximate calculation for the admittance seen looking into a slot in the shield of a multiconductor transmission line when a uniform magnetic current is placed over the slot. The calculation presented is approximate in that only the transmission line mode was used in the calculation; all higher order waveguide modes were neglected. By neglecting the higher order waveguide modes the magnetic current may be replaced by a point voltage source at the slot location. The admittance calculation then corresponds to calculating the driving point admittance of a point voltage source located in the shield of an MTL.

References

[1] R. G. Plumb, R. F. Harrington, and A. T. Adams, "An electromagnetic model for multiconductor connectors," *IEEE Trans. Electromagn. Compat.*, vol. 32, pp. 38–52, Feb. 1990.

[2] R. G. Plumb and R. F. Harrington, "The electromagnetic response of a multiconductor connector," Report TR-88-15, Syracuse Univ., Syracuse, NY, 1988.

[3] C. R. Paul, "Useful matrix chain parameter identities for the analysis of multiconductor transmission lines," *IEEE Trans. Microwave Theory Tech.*, vol. MTT-23, pp. 756–760, Sept. 1975.

[4] N. Balabanian and T. Bickart, *Linear Network Theory*. Beaverton, OR: Matrix, 1981.

Full-Wave Analysis of Multilayer Coplanar Lines

Chia-Nan Chang, Wen-Chang Chang, and Chun Hsiung Chen

Abstract—**A full-wave analysis of a coplanar wave-guiding structure with multiple dielectric layers is presented. In this study, the results of the hybrid approach that combines the finite-element method and the conformal-mapping technique are compared with those of the spectral-domain approach. Numerical results for effective dielectric constants, characteristic impedances, current distributions, and field distributions for various multilayer coplanar line structures are presented and discussed. Comparisons are also made of the computed results with the available quasi-static ones.**

I. Introduction

With the increased use of suspended substrate lines and for special purposes such as protection from mechanical or chemical damage and the provision of additional means to adjust the transmission line characteristics, the study of multilayer planar wave-guiding structures has received the attention of a number of investigators [1]–[5]. Instead of analyzing the problem directly in the space domain, most previous work has been carried out in the spectral domain. Rapidity in obtaining the dispersion characteristics of the lines is an advantage of this technique. However, it is not so easy to obtain both the field patterns and the characteristic impedances of multilayer planar wave-guiding structures because of the complicated mathematical manipulation of the fields from the spectral domain to the space domain.

In a recent investigation, a rigorous hybrid full-wave analysis of coplanar waveguide is presented [6]. In that work, the infinite space in the original domain is first mapped into a finite region in the image domain by the mapping function originally employed by Wen [7]. The transformed variational equation in the image domain is then solved efficiently by the conventional finite-element method. In this way, the difficulties associated with both the infinite space and the field singularity near the conductor edges can be removed. In this paper, the same hybrid approach is utilized to study the full-wave characteristics of a coplanar line structure with multiple dielectric layers. Especially, the frequency-dependent effective dielectric constants and characteristic impedances of the multilayer coplanar line are calculated and compared with available data [4], [5]. Also investigated are the field distribution along the center line of the slot and the current distributions on both the signal strip and the ground plane. Because of a lack of data for comparison, the results of this hybrid approach are validated by a comparison with those of the spectral-domain approach [5].

Manuscript received May 17, 1990; revised November 5, 1990. This work was supported by the National Science Council, Republic of China, under Grant NSC 79-0404-E002-39.

The authors are with the Department of Electrical Engineering, National Taiwan University, Taipei 10764, Taiwan, Republic of China.

IEEE Log Number 9042503.

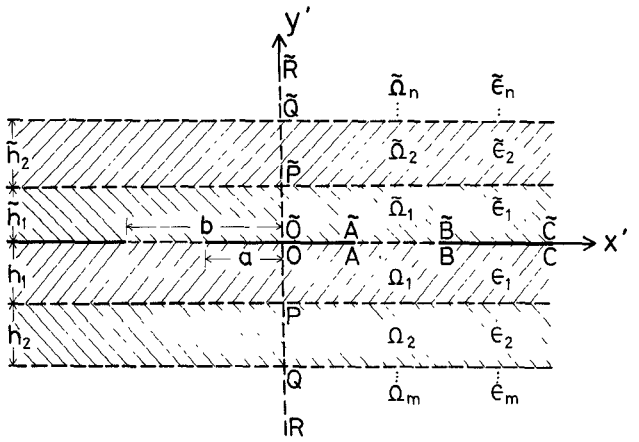

Fig. 1. Geometry of mulilayer coplanar line and original domain ($x' \geq 0$) in z' plane.

II. Formulation

Consider an open uniform coplanar line structure with multiple layers of isotropic and lossless dielectrics as shown in Fig. 1. Here a central metal strip (assuming negligible thickness) of width $2a$ and two conducting ground planes (also of negligible thickness) of separation $2b$ are placed in the plane ($y'=0$) between dielectric layers. Above and below the conductors are n upper and m lower homogeneous dielectric layers of permittivities $\tilde{\epsilon}_k = \epsilon_0 \tilde{\epsilon}_{rk}$ ($k=1,2,\cdots,n$) and $\epsilon_k = \epsilon_0 \epsilon_{rk}$ ($k=1,2,\cdots,m$), respectively. The guided modes of this inhomogeneous structure are in general hybrid; therefore, both the axial components E_z and H_z are required in the analysis. As far as the fundamental (E_z even and H_z odd) mode is concerned, it is sufficient to consider the right half structure with a magnetic wall at $x'=0$.

A. Hybrid (Finite-Element / Conformal-Mapping) Approach

Following the idea of [6], Wen's mapping function [7]

$$z' = a\,\mathrm{sn}(z,k) \tag{1}$$

is used to map the right half plane $x' \geq 0$ (original domain) in Fig. 1 into a rectangular region (of width $2K(k)$ and height $K(k')$) in the image domain (Fig. 2). Here, $\mathrm{sn}(z,k)$ is the complex sine elliptic function, $K(k)$ and $K(k')$ are the complete elliptic integrals of the first kind and the second kind [8], $k = a/b$, and $k' = \sqrt{1-k^2}$. By this mapping, the transverse fields $(\vec{E}_t, \vec{H}_t)$ are smooth everywhere in the image domain [6], although the transverse fields $(\vec{E}_t', \vec{H}_t')$ in the original domain exhibit edge singularity near the conductor edges. Thus the field singularity difficulty in the original domain may be removed.

The variational formulation for the multilayer coplanar lines in the image domain (Fig. 1) is the same as [6, eq. (1)], and the boundary conditions on the electric and magnetic walls are shown in Fig. 2. The details of the numerical procedures are given in [6].

B. Spectral-Domain Approach

For purposes of cross checking, the new type of spectral-domain approach [9] is also applied to the multilayer coplanar

0018-9480/91/0400-0747$01.00 ©1991 IEEE